Earthquake Engineering, Tenth World Conference © 1992 Balkema, Rotterdam. ISBN 90 5410 060 5

Evaluation of the maximum strength of H-shaped steel beam-to-column connections

A. Matsuo, Y. Nakamura & R.W. Salib
Hiroshima University, Japan
Y. Mukudai & T. Takamatsu
Hiroshima Institute of Technology, Japan

ABSTRACT: An experimental study to know the ultimate strength of H-shaped steel beam-to-column welded connection is performed. Depending upon the experimental observations and data, the deformed configurations of two collapse mechanisms are suggested and a formulation of the collapse load for each mechanism taking into account the axial deformation of the beam flange is developed. A comparison of the ultimate strength between the experimental and evaluated results of X and T-types subassemblages is achieved.

1 INTRODUCTION

In the current aseismic design of steel structures in Japan, it is assumed that beam-to-column connection shares approximately one-third of the total energy absorbed by the whole frame. However, experimental results exhibit that the connection has a considerable ability to absorb energy more than the assumed value (Architectural Institute of Japan A.I.J. 1990.9). Nakao (1981.2) suggested that the beam-to-column subassemblage whose connection is designed weaker than beams and columns has an adequate energy absorption capacity to make use of it for the aseismic design of steel structures. To establish this design, the formulation of ultimate strength of the connection is indispensable. In this paper, six specimens of X-type H-shaped steel beam-to-column connections of various panel yield strengths are tested until the ultimate strength is obtained. Based on the philosophy of Limit Analysis, two collapse mechanisms for the connection are suggested and the collapse load of each is evaluated considering the effect of axial deformation in the beam flange. A comparison of ultimate strength between experimental and predicted results is achieved. In addition, this formulation is applied to various types of subassemblages and two-bay two-story frames which have been tested by others.

2 EXPERIMENTAL STUDY

The specimens are divided into two groups. The sections H-200*160*9*12 and H-180*180*9*16 are used for beams and columns of the first group respectively (specimens XMC0-3-0617, XMC0-4-0617 and XMB0-5-0617), while the sections H-300*160*9*12 and H-180*180*9*12 are used for those of the second group (specimens XMC0-3-0818, XMC0-4-0818 and XMC0-5-0818). In the first group, the depth of beams is constant of 200 mm, while it increases to 300 mm in the second one. The aim of varying the beam depth from one group to another is to distinguish between two kinds of collapse mechanisms which are explained in the following section. In each group, the panel thickness is only the unique parameter and changes from 12 to 25 mm in the first group and from 9 to 16 mm in the second one. The purpose of changing panel thickness is to obtain various values of panel yield ratio R_{PY}, where R_{PY}=panel yield moment/ column or beam yield moment whichever is smaller. The experimental specimen and the welded joint detail are illustrated in Fig.1. The sizes of specimens and the mechanical properties are listed in Tabs.1 and 2 respectively.

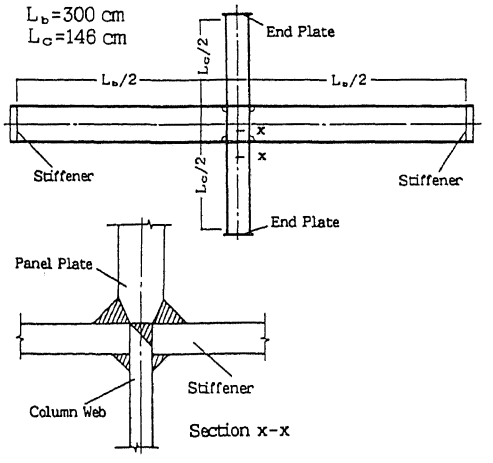

Fig.1 Experimental specimen and detail of welded joint

Table 1. Size of experimental specimens

Specimen	XMC0-3-0617	XMC0-4-0617	XMB0-5-0617
Panel plate thickness (mm)	12	19	25
Panel yield ratio	0.27	0.39	0.52
Material number of column flange	11	11	11
column web	2	2	2
beam flange	8	8	8
beam web	1	1	1
panel plate	9	12	13

Specimen	XMC0-3-0818	XMC0-4-0818	XMC0-5-0818
Panel plate thickness (mm)	9	12	16
Panel yield ratio	0.37	0.44	0.54
Material number of column flange	7	7	7
column web	5	5	5
beam flange	8	8	8
beam web	4	4	4
panel plate	3	6	10

Table 2. Mechanical properties

Material number	1	2	3	4	5	6	7
Thickness (mm)	9	9	9	9	9	12	12
Yield stress (tonf/cm²)	3.27	3.29	3.20	3.29	3.17	2.87	2.86
Ultimate stress (tonf/cm²)	4.52	4.56	4.50	4.53	4.51	4.50	4.44

Material number	8	9	10	11	12	13
Thickness (mm)	12	12	16	16	19	25
Yield stress (tonf/cm²)	2.86	2.83	2.61	2.67	2.57	2.60
Ultimate stress (tonf/cm²)	4.44	4.45	4.28	4.32	4.27	4.38

3 EXPERIMENTAL AND FINITE ELEMENT RESULTS

3.1 Load-deflection relation

P-δ and P-$_P\delta$ relations are plotted in Fig.2. δ is the total displacement of the loading point and $_P\delta$ is the displacement due to panel deformation. It can be noticed that in the plastic range, the panel deformation becomes larger and it reaches to 65%~ 70% of the total deformation at the ultimate state. Also, numerical P-δ relations for two specimens (XMB0-5-0617 and XMC0-3-0818) calculated by Finite Element Method are presented in the same figure.

3.2 Curvature distribution along the column flange

Fig.3 illustrates the curvature distribution along the column flange at the panel. Horizontal axis indicates the locations of measured curvatures on the column flange starting from the intersection point of flanges. It can be observed that, for specimen XMC0-3-0617 (Fig.3-a), curvature close to

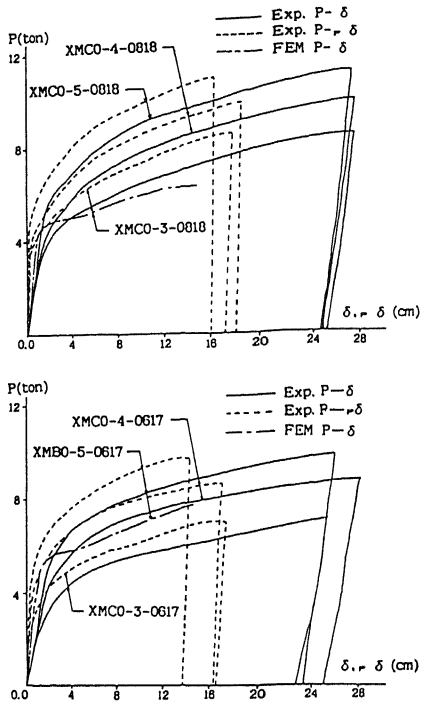

Fig.2 P-δ and P-$_P\delta$ relations

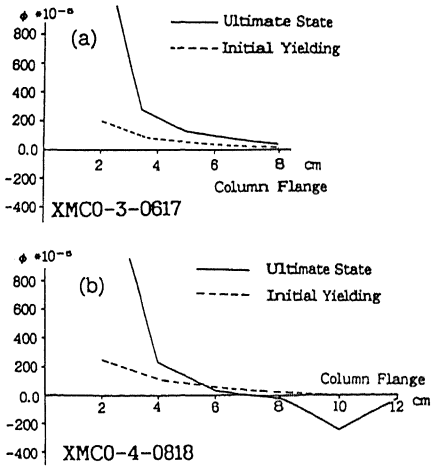

Fig.3 Curvature distribution along the column flange

the intersection of flanges is large and lastly reaches to the ultimate state with only one plastic hinge close to the intersection of flanges. On the contrary, for specimen XMC0-4-0818 (Fig.3-b), curvature far from the intersection of flanges becomes also large. These two kinds of distributions suggest the deformed configurations of collapse mechanisms for the two cases of small and large beam depths respectively. Furthermore, moment distributions along the flanges surrounding the panel

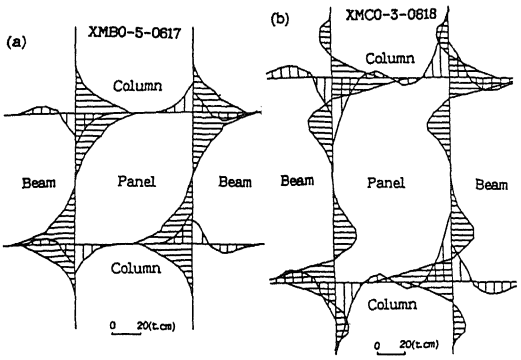

Fig.4 Moment distribution along flanges

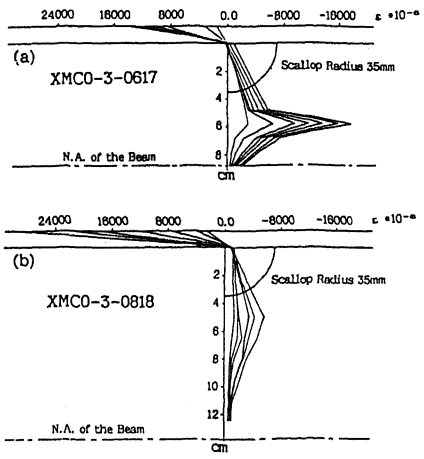

Fig.5 Strain distribution along the beam web

calculated by Finite Element Method also emphasize the positions of plastic hinges of the collapse mechanisms in the two cases (Fig.4-a and b).

3.3 Distribution of plastic regions within the connection

Strain distribution along the section of the beam web close to the connection is illustrated in Fig.5. Moreover, the plastic regions within the connection are predicted using Finite Element Method and illustrated in Fig.6-a and b. These experimental and evaluated results suggest the collapse mechanisms which the authors are going to explain in the following section.

4 LIMIT ANALYSIS

Depending upon the experimental observations and numerical results, the deformed configurations of two collapse mechanisms considering the axial

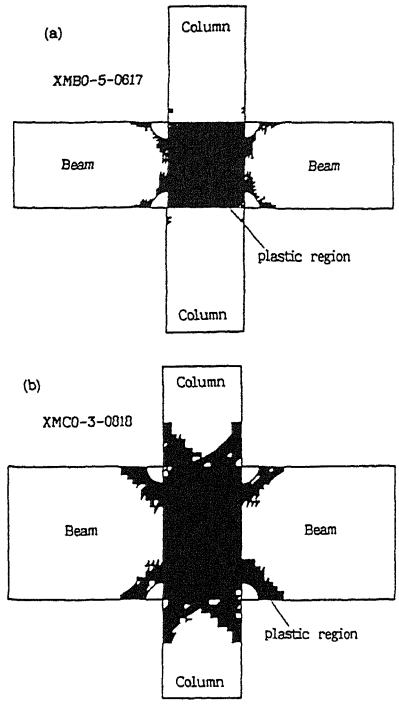

Fig.6 Plastic regions at the connection

deformation of the beam flange are presented in Fig.7. The flanges are assumed to be line elements. If the depth of beam is large, the collapse mechanism 3 is possible. On the contrary, for the beam of small depth, the probability of forming two plastic hinges in the column flange at each corner of the connection becomes smaller as half of the beam depth is less than a+b where a is the size of the rigid part and b is the distance between the two plastic hinges. Consequently, the collapse mechanism 4 becomes dominant. Based on Limit Analysis strategy, an analytical formula to estimate the collapse load of each mechanism is deduced. Moment - axial force interaction is also taken into consideration and expressed by the following equation:

$$M_{ubf}' = M_{ubf}\{1-(N/N_{ubf})^2\} \quad (1)$$

where M_{ubf} and M_{ubf}' are the ultimate moment and the reduced ultimate moment of the beam flange respectively, N and N_{ubf} are the actual and ultimate axial forces of the beam flange. The collapse load of the mechanism 3 is given by the following equation:

$$P=[S*a(a+b-c)^2/b+2.6M_{ubf}'+2(1.3M_{ubf}'+M_{Pbf})*a/b+5.2M_{ubf}*N^2(1+a/b)/N_{ubf}^2+2*\{0.5S*(a+b-c)^2+1.3M_{ucf}+M_{Pcf}\}*\{a-2.6M_{ubf}*N*(1+a/b)(1-2(a+b)/{}_bH)/N_{ubf}^2\}/b-5.2SM_{ubf}*N*(1+a/b)(a+b-c)^2/(N_{ubf}^2*{}_bH)+2.6M_{ucf}+0.5\tau_u*{}_cH*{}_bH*t_{PP}]/[l_b*(1-{}_cH/l_b-{}_bH/l_c)/2+2.6M_{ubf}*N*(1+a/b)*(l_b-{}_cH)/(N_{ubf}^2*{}_bH)] \quad (2)$$

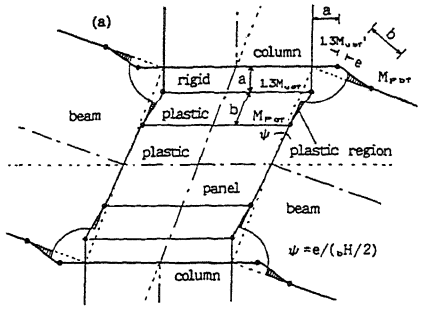

Collapse Mechanism 3

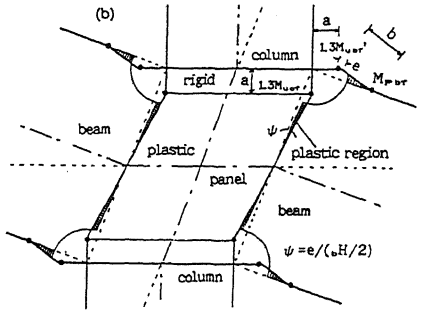

Collapse Mechanism 4

Fig.7 Collapse mechanism

Table 3. A comparison of ultimate strength between experimental and analytical results

Specimen	XMC0-3-0617	XMC0-4-0617	XMB0-5-0617
Experimental ultimate strength (tonf)	7.00	8.71	9.72
Collapse load of mechanism 1 (tonf)	6.83	8.97	11.04
mechanism 2 (tonf)	6.67	8.81	10.89
mechanism 3 (tonf)	6.55	8.52	10.38
mechanism 4 (tonf)	6.40	8.35	10.20
Beam collapse load P_{Pb} (tonf)	10.99	10.99	10.99
Column collapse load P_{Pc} (tonf)	8.94	8.94	8.94

Specimen	XMC0-3-0818	XMC0-4-0818	XMC0-5-0818
Experimental ultimate strength (tonf)	8.20	9.75	11.03
Collapse load of mechanism 1 (tonf)	7.52	9.22	11.15
mechanism 2 (tonf)	7.70	9.40	11.53
mechanism 3 (tonf)	7.31	8.92	10.74
mechanism 4 (tonf)	7.42	9.02	10.82
Beam collapse load P_{Pb} (tonf)	10.16	10.16	10.16
Column collapse load P_{Pc} (tonf)	15.22	15.22	15.22

N and b are determined by the following two conditions:

$$dP/dN=0 \quad \text{and} \quad dP/db=0 \tag{3}$$

where l_b, l_c and $_bH$, $_cH$ are beam and column lengths and depths respectively, c is the scallop radius, S is the yield strength of the beam web calculated from Von Mises yield criterion or the punching shear strength of the flange or strength of the fillet weld *between flange and web whichever is smaller*, M_{Pbf} and M_{Pcf} are the plastic moments of beam and column flanges respectively, M_{ucf} is the ultimate moment of the column flange, τ_u is the ultimate shear stress of the panel plate and t_{PP} is the panel plate thickness. In the same manner the following equation is derived for the collapse mechanism 4:

$$P=[S*a(a+b-c)^2/b+2.6M_{ubf}'+2(1.3M_{ubf}'+M_{Pbf})*a/b+5.2M_{ubf}*N^2*(1+a/b)/N_{ubf}^2+0.5S*{}_bH(1-2c/{}_bH)^2*\{a*{}_bH/({}_bH-2a)-2.6M_{ubf}*N*(1+a/b)/N_{ubf}^2\}+2.6*M_{ucf}*\{1+2a/({}_bH-2a)\}+0.5\tau_u*{}_cH*{}_bH*t_{PP}]/[l_b*(1-{}_cH/l_b-{}_bH/l_c)/2+2.6M_{ubf}*N*(1+a/b)*(l_b-{}_cH)/(N_{ubf}^2*{}_bH)] \tag{4}$$

N and b are determined also from equation (3). If the axial deformation of beam flanges is ignored, e in Fig.7 becomes zero. Therefore, the mechanisms 3 and 4 convert to the mechanisms 1 and 2 respectively. Consequently, the collapse load of the mechanism 1 is given by the following equation:

$$P=[4S*a(a+b-c)^2/b+5.2(1+a/b)(M_{ubf}+M_{ucf})+4a(M_{pbf}+M_{pcf})/b+\tau_u*{}_cH*{}_bH*t_{PP}]/[l_b(1-{}_cH/l_b-{}_bH/l_c)] \tag{5}$$

where

$$b=\sqrt{[(a-c)^2+(1.3M_{ubf}+M_{pbf}+1.3M_{ucf}+M_{pcf})/S]} \tag{6}$$

Also the following equation is derived for the mechanism 2:

$$P=[2S*a(a+b-c)^2/b+5.2M_{ubf}(1+a/b)+4M_{pbf}*a/b+\{S*a({}_bH-2c)^2+5.2M_{ucf}*{}_bH\}/({}_bH-2a)+\tau_u*{}_cH*{}_bH*t_{PP}]/[l_b(1-{}_cH/l_b-{}_bH/l_c)] \tag{7}$$

where

$$b=\sqrt{[(a-c)^2+2(1.3M_{ubf}+M_{pbf})/S]} \tag{8}$$

5 A COMPARISON OF ULTIMATE STRENGTH BETWEEN EXPERIMENTAL AND CALCULATED RESULTS

5.1 In-door specimens

The experimental and predicted results which have been deduced on the basis of estimated collapse *mechanisms for the inspected subassemblages are* listed in Tab.3. Fig.8 presents a plot of the collapse load against panel yield ratio R_{Pv} for these subassemblages. It can be noticed that the evaluated ultimate strength of the connection (the minimum collapse load) predicts the experimental one well. In the case of a small beam depth, the collapse mechanisms 2 and 4 give smaller collapse loads than those of mechanisms 1 and 3. On the other hand,

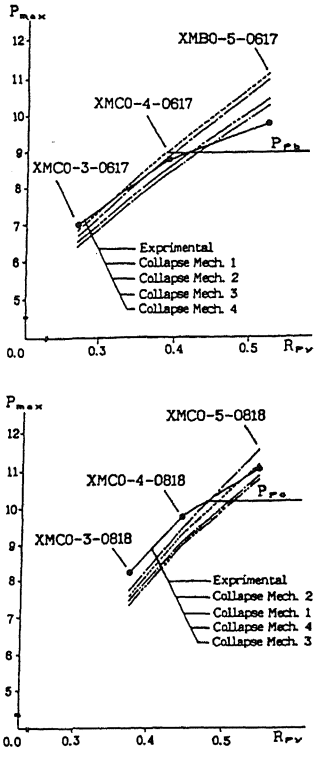

Fig.8 Collapse load

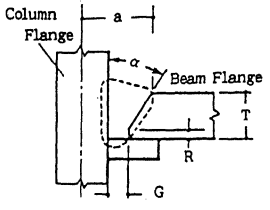

T	G	R	α
≧6	6	2	45°
≧12	9	2	35°

Fig.9 Size of the rigid part a

when the depth of the beam becomes larger, the collapse mechanisms 1 and 3 give smaller values than those of 2 and 4. The collapse mechanism considering the axial deformation of beam flanges gives a smaller strength than that of neglecting it. However, the increasing of the collapse load due to the neglecting of the axial deformation in the beam flange is insignificant. Also, from Fig.8 it can be noticed that for specimens XMB0-5-0617 and XMC0-5-0818, plastic hinges are formed within the beams or columns cross sections before the connection reaches the ultimate strength, where P_{Pb} and P_{Pc} are the loads corresponding to the plastic moments of beam and column cross-sections respectively.

Table 4. A comparison of ultimate strength between experimental and analytical results for many recorded data a : X-type

Specimen number	24	117	118	120	123	124	126	127	128
Panel yield ratio	.35	.31	.48	.45	.63	.61	.43	.59	.36
Experimental ultimate strength (tonf)	14.9	7.9	8.1	12.8	9.1	11.7	9.4	15.8	12.3
Collapse load of									
mechanism 1 (tonf)	17.34	9.23	9.49	12.9	10.84	12.25	11.42	16.36	13.24
mechanism 2 (tonf)	17.51	9.41	9.71	13.12	11.06	12.47	11.55	16.50	13.31
mechanism 3 (tonf)	16.87	9.03	9.26	12.56	10.58	11.92	11.19	15.95	12.97
mechanism 4 (tonf)	16.88	9.15	9.45	12.68	10.72	12.05	11.28	16.01	13.00

Specimen number	129	131	134	142	147	148	149	151	ZO
Panel yield ratio	.54	.63	.61	.46	.28	.28	.23	.28	.81
Experimental ultimate strength (tonf)	16.8	28.75	17.96	35.0	14.23	10.40	7.95	6.86	39.30
Collapse load of									
mechanism 1 (tonf)	18.72	28.19	17.19	34.19	13.87	9.37	6.97	6.87	35.29
mechanism 2 (tonf)	18.79	25.89	17.08	34.46	13.79	9.35	7.00	6.95	34.48
mechanism 3 (tonf)	18.26	25.21	16.38	32.95	13.47	9.06	6.84	6.82	.....
mechanism 4 (tonf)	18.27	25.35	16.50	32.99	13.32	8.98	6.86	6.88	.....

b : T-type

Specimen number	1	2	5	9	91	92	93	94
Panel yield ratio	.37	.37	.95	.79	.83	.83	.83	.83
Experimental ultimate strength (tonf)	6.25	7.11	5.88	8.28	10.10	10.00	8.90	10.35
Collapse load of								
mechanism 2 (tonf)	7.10	7.10	6.31	8.97	9.41	9.41	9.41	9.41
mechanism 4 (tonf)	7.00	7.00	6.25	8.83	9.3	9.30	9.3	9.30

Specimen number	95	102	103	104	107	138	150
Panel yield ratio	.63	.45	.68	.68	.68	.92	.44
Experimental ultimate strength (tonf)	9.85	2.9	1.84	3.3	1.75	65.3	11.5
Collapse load of							
mechanism 2 (tonf)	9.41	2.78	1.78	3.3	1.78	63.5	10.57
mechanism 4 (tonf)	9.3	2.8	1.72	3.2	1.72	63.48	10.47

5.2 Predicted ultimate strength for other experimental data

The authors applied the developed collapse mechanisms to other experimental specimens which have been done by many investigators in Japan (A.I.J. 1990.9, Nakao 1981.2)and calculated the collapse loads. Some of these specimens are X-type and the others are T-type H-shaped steel welded connections. The size of rigid part a is determined by the specifications of the shapes and sizes of welded grooves (A.I.J. 1987) and illustrated in Fig.9. The experimental and analytical results are listed in Tab.4-a, and b. It can be noticed that the analytical results predict the experimental maximum strength well. Moreover, even though some of these specimens do not have scallops, the developed formula for the specimens with scallops gives a good prediction to the experimental results. Also, increasing of the collapse load due to ignoring the axial deformation of the beam flange is inconsiderable. Therefore, for simplicity, the collapse mechanisms 1 and 2 are applicable without a substantial error.

5.3 Collapse load for two-bay two-story frame

Experimental results of two frames which were tested by Nakao (1981.2) are adopted. In these results, P-δ

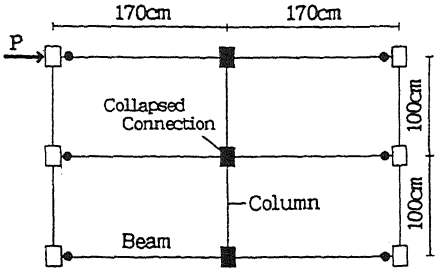

Fig.10 Collapse mechanism of two- bay two-story Frame

Tab.5 A comparison of ultimate strength of frames between experimental and calculated results

Specimen	F-2A(c)	F-2B(c)
Beam	H-200*100*5.5*8	H-200*100*6*12
Column	H-150*150*7*10	H-150*150*6*12
Experimental ultimate strength (tonf)	29.42	49.80
Evaluated ultimate strength (tonf)	29.98	42.65

effect of columns' axial loads decreased the experimental ultimate strength of the frame. In order to satisfy the comparison between experimental and predicted results, this effect is excluded. The collapse mechanism of the whole frame is assumed to be as shown in Fig.10. Based on the principles of Virtual Work and using the suggested collapse mechanism of the connection, the ultimate load of the frame is calculated and compared with the experimental one. The results are listed in Tab.5. It can be observed that the predicted results follow the experimental ones well.

6 CONCLUSIONS

Six specimens of X-type H-shaped steel beam-to-column connections of different values of R_{Pv} are selected and tested until the ultimate strength for each one is achieved. On the basis of these experimental and numerical results, the collapse mechanisms of the whole connection are presented. A comparison of the ultimate strength between experimental and analytical results is performed. From this study the following conclusions are drawn:

1. The suggested collapse mechanisms give satisfactory results to the authors' experimental data.

2. The proposed formula exhibits a good prediction to the experimental results of X and T-types carried out by other researchers.

3. The increasing of collapse load due to the neglecting of axial deformation in the beam flange is inconsiderable. Consequently, for simplicity ,the collapse mechanisms 1 and 2 can be used without a significant error.

7 REFERENCES

A.I.J., 1990.9. "Symposium on the behavior of steel beam-to-column connections and problems in practical design", Japan.

A.I.J., 1987. "Technical recommendations of steel construction for buildings, Part 1 Guide to steel-rib fabrications", Japan.

Matsuo, A., Salib, R.W., Mukudai, Y., Takamatsu, T. and Shinabe, Y., 1991.3. "A study to formulate the restoring force characteristics of H-shaped steel beam-to-column connection", Journal of Structural Engineering, Vol.37B, PP. 283-294, Japan.

Matsuo, A., Salib, R.W., Mukudai, Y., Takamatsu, T. and Yasaka, H., 1991.9. "A study on the maximum strength and restoring force characteristics of H-shaped steel beam-to-column subassemblage", Part 1, 2, Proc. of Annual Meeting of A.I.J., PP. 1151-1154

Mukudai, Y., Matsuo, A., Shinabe, Y., Takamatsu, T. and Salib, R.W.,1990.3. "A study on the evaluation of maximum strength of H-shaped steel beam-to-column connections with a weak panel" Part 1, Journal of Structural Engineering, Vol. 36B, PP. 341-348, Japan.

Mukudai, Y. and Matsuo, A., 1987.5. " A study on load carrying capacity and plastic deformation capacity of beam-to-column connections composed of H-shaped members made of comparatively thin plates", Part 1, Transactions of . A.I.J., No. 375, PP.43-52.

Naka, T., Nakao, M. and Osano, H., 1981.2. "Restoring force characteristics of steel beam-to-column connections and aseismicity of frames", The 27th Symposium on Structural Engineering, Japan.